NANOSYSTEMS: PHYSICS, CHEMISTRY, MATHEMATICS, 2016, 7 (3), P. 451–458

Synthesis and study of anhydrous lanthanide orthophosphate (Ln = La, Pr, Nd, Sm) nanowhiskers

K. I. Bryukhanova, G. E. Nikiforova, K. S. Gavrichev

Kurnakov Institute of General and Inorganic Chemistry of the Russian Academy of Sciences, Leninsky prospect 31, Moscow, 119991, Russia

bryuhanova@igic.ras.ru

PACS 61.46.-w, 81.20.-n **DOI 10.17586/2220-8054-2016-7-3-451-458**

The effect of hydrothermal synthetic conditions on the obtaining of lanthanide orthophosphates $LnPO_4$ (Ln = La, Pr, Nd, Sm) with different structure, size and shape of particles was revealed. The optimum conditions for preparation of anhydrous nanoscale lanthanide orthophosphates with monoclinic structure were determined. The prepared nanowhiskers had lengths ranging from 0.4 μm (for $LaPO_4$) to 5 μm (for $SmPO_4$), and the diameter – from 30 nm (for $LaPO_4$) to 200 nm (for $SmPO_4$). The size of particles synthesized under similar conditions increased with decreased of lanthanide ion radius.

Keywords: nanowhisker, lanthanides, orthophosphates, hydrothermal synthesis, size factor.

Received: 12 February 2016

1. Introduction

A preparation of inorganic materials containing nanosized particles (up to 100 nm) with a geometrical dimension below 3 is the actual task of the modern materials science. Nanoscale substances' properties, such as electronic, optical, chemical, thermal and mechanical properties [1–6] differ sufficiently from those of the bulk phase material. Usually, nanoparticles contain a significant quantity of substances adsorbed on their surface and the measurement of its own properties (in part, thermal and thermodynamic) is difficult. So the necessity arises to elaborate experimental routes for the synthesis of nanocrystalline substances without detectable amounts of adsorbed impurities.

Lanthanide orthophosphates of cerium subgroup (Ln = La – Gd) can be found in nature in the form of crystal hydrates $LnPO_4 \cdot (x + 0.5)H_2O$ [7] with hexagonal structure (space group $P6_222$, mineral rhabdophane) or in the anhydrous form $LnPO_4$ with the monoclinic structure (space group $P2_1/c$, mineral monazite) [8, 9].

Lanthanide orthophosphates with these structures can be synthesized in the laboratory by different methods: a precipitation from the solutions, a sol-gel technique, a hydrothermal synthesis, a solid state reaction (ceramic method) [14], as well as by the application of microwave [10], sonochemical [11, 12] and mechanical treatments (high-energy milling) [13].

The precipitation from solutions and sol-gel methods allow preparation of mostly hexagonally-structured crystalline substances with the isometric micro- [15, 16] and nanoparticles [17, 18]. In rare instances an amorphous phase [19–21] or nanowhiskers [16] can also be obtained by above-mentioned ways. Subsequent sintering of these samples at temperatures above 700 °C leads to the formation of an anhydrous monoclinic phase [17, 19, 20, 22]. Moreover, it is noted that annealing can cause an increase in the particle size [23] that does not permit one to unambiguously attribute measured properties to nanoscale crystals. According to a literature review, the hydrothermal method is preferable for the synthesis of lanthanide orthophosphates with low-dimensional particles (the particles for whose the size in one direction is sufficiently larger than in the remaining directions), because this method makes it possible to obtain the completely uniform particles size avoiding an additional high-temperature sintering and a multi-stage treatment. By varying the hydrothermal synthesis parameters (temperature and time of treatment, ratio of initial reagents, pH), one can promote a preparation of final products with the controlled chemical composition, dimension, morphology and crystal structure.

The ratio of initial reagents, including a rare earth cation and a phosphate anion plays a key role in the phosphorous coordination generation [21] and, as a consequence, allows one to adjust the composition [20, 24] and morphology [16, 25] of the forming phase. An excess of phosphorous in the reagent mixture always leads to polyphosphates formation, and for this reason, an equimolar ratio of La:P is optimal for the preferred orthophosphate synthesis. Different compounds H_3PO_4, $NH_4H_2PO_4$, $Na_3PO_4 \cdot 12H_2O$, P_2O_5, organic compounds [26] are usually used as the phosphate group containing precursors.

The pH value plays a significant role in the formation of the final product, since it has an impact not only on the phase composition of the product, but also on the preferential growth of particles in one direction or

another [27]. It was noted [1, 28–30] that an increasing of pH value from 0 to 10 leads to the change of a particle shape from nanowhiskers to isometric nanoparticles and, moreover, to the formation of rare earth (RE) hydroxide impurities [8, 28, 31]. The pH value near 1 leads to the formation of unidimensional structure samples.

A great deal of attention in the literature is devoted to the influence of synthetic parameters on the phase composition and the morphology of the obtained particles, however, this information is fragmented. Thus, authors [1, 6, 8, 25, 29, 34] describe the influence of the synthesis temperature not only on the phase composition (hexagonal or monoclinic phase), and also on the change of the shape and dimension of the particles. While the influence of hydrothermal processing time on the final phase composition is described in articles [25, 32], the information regarding the morphology changes in the particles is missing. In [33], only the effect of synthesis time on particle size of the obtained substances is reported.

The goal of this research is the elaboration of a synthesis route to one-dimensional anhydrous cerium subgroup lanthanide orthophosphates (nanowhiskers) for subsequent studies of its thermal and thermodynamic properties.

2. Experimental

2.1. Synthesis

High-purity RE oxides La_2O_3, Pr_6O_{11}, Nd_2O_3, Sm_2O_3 (99.99 mass%), ammonium dihydrogenphosphate $NH_4H_2PO_4$ ("pure for analysis" grade), hydrochloric acid ("pure" grade) concentration 34.68 mass% and distilled water were used as the initial reagents.

RE Oxides were dissolved in hydrochloric acid and mixed with ammonium dihydrogenphosphate in a 1:1 Ln:P ratio. Hydrothermal synthesis was conducted under "soft" conditions, varying the temperature (120 °C, 160 °C and 200 °C) and time of processing (55 and 100 hours) in a stainless steel autoclave with Teflon liner ($V = 7$ mL). The autoclave filling coefficient was 0.75 – 0.80 and pH = 0 – 1. The rate of cooling after hydrothermal treatment to temperatures of 40 – 60 °C was ~ 1 °C/min. The obtained sediments were washed with distilled water from mother liquor at room temperature using the blue tape ash-free filters and was then aerobically dried at 80 °C for 6 h.

2.2. Samples characterization

X-ray powder diffraction (XRD) patterns were performed on a BrukerAdvance D8 diffractometer (Cu Kα_{cp} radiation, $\lambda = 1.5418$ Å, reflection geometry, $2\theta = 10 - 60$ degree, step 0.02).

The size and morphology of the formed particles were evaluated by the scanning electron microscopy (SEM) CrossBeam Zeiss NVision 40 ($U = 1$ kV).

The water content and the thermal stability of the lanthanide orthophosphates were studied by differential scanning calorimetry and thermogravimetric analysis (DSC/TG) using Netzsch STA 449F1 Jupiter® in the inert gas (helium 6.0) flow.

The surface specific area of powder was determined by low-temperature nitrogen adsorption method in ATX_06 Katakonusing the BET model.

3. Result and discussion

Synthesis parameters, structure type and particles size of the lanthanide orthophosphates with the general formula $LnPO_4$ (Ln = La – Sm) are presented in Table 1. The XRD patterns of the $LnPO_4$ samples prepared at 200 °C/55 h by hydrothermal method are shown in Fig. 1.All reflections can be readily indexed to a pure monoclinic phase (space group $P2_1/c$) and are in agreement with data for RE orthophosphates from ICCD PDF2 (JCPDS 84-0600, 83-0653, 83-0654 and 46-1329 for orthophosphates of La, Pr, Nd and Sm, respectively). But hexagonal phase peaks are also detected in diffractograms of the $LaPO_4$ and $PrPO_4$ samples synthesized at 120 °C and 160 °C (these data are not shown). The peak shapes shows that the samples were well-crystallized. Unit cell parameters calculated from X-ray patterns are given in Table 2. There are only unit cell parameters for isometric particles or single crystals of La, Pr, Nd and Sm orthophosphates in the literature. Comparison of crystallographic characteristics for particles with different morphologies allows one to understand the nucleation process better. As is shown in the Table 2, the parameters a, b and angle β is slightly larger for nanowhiskers than what is typical for anisotropic crystal growth [8, 27].

Figure 2 displays the thermal behavior for monoclinic $LnPO_4$ (Ln = La, Pr, Nd, Sm) nanowhiskers obtained at 200 °C/55 h. All samples were shown to not contain adsorbed water and volatile impurities. Specimens synthesized at 120 °C and 160 °C (La4, Pr3 and Pr4) contain a small amount of water, which confirms the presence of hexagonal phase substances in the final product (data are not given). These results are in good agreement with the results of XRD.

TABLE 1. Synthesis conditions (pH = 0 – 1), crystal structures and morphology of $LnPO_4$ (Ln = La, Pr, Nd and Sm) nanowhiskers

Sample	t, °C	τ, h	Crystal system*	Particle size, μm (length/diameter)	S_{surf}, m^2/g
$LaPO_4$					
La1	200	55	M	0.5 – 0.7 / 0.045	12.0
La2	200	100	M	0.4 – 0.6 / 0.08 – 0.10	8.9
La3	160	55	M	0.6 – 0.8 / 0.05	—
La4	120	55	M + H	—	—
$PrPO_4$					
Pr1	200	55	M	1.0 – 1.5 / 0.03 – 0.06	15.7
Pr2	200	100	M	1.0 – 2.0 / 0.05 – 0.10	11.0
Pr3	160	55	M + H	0.2 – 2.0 / 0.04 – 0.09	—
Pr4	160	100	M + H	—	—
$NdPO_4$					
Nd1	200	55	M	0.2 – 2.0 / 0.05	19.9
Nd2	200	100	M	0.8 – 1.5 / 0.04 – 0.10	9.3
Nd3	160	100	M	—	—
$SmPO_4$					
Sm1	200	55	M	1.0 – 5.0 / 0.12 – 0.25	4.9
Sm2	200	100	M	0.8 – 3.0 / 0.12 – 0.25	5.3
Sm3	160	100	M	—	—
*M – monoclinic form, H – hexagonal form.					

The average size of particles presented in Table 1 is determined from SEM images. Figs. 3–6 show the particles have the shape of whiskers with diameter from 30 nm (for La-, Pr- and $NdPO_4$) to 120 nm (for $SmPO_4$) and length up to several microns.

Increasing the hydrothermal treatment time leads to particle growth and, as a consequence, a decreasing in the surface area (Table 1, Figs. 3–6). This is a typical for La1 and La2, Pr1 and Pr2, Nd1 and Nd2 samples. The exception is samarium orthophosphate, whose particles are larger in diameter and their size doesn't appreciably change with prolonged treatment time.

The analysis of obtained data shows that decreased treatment temperature results in the formation of a biphasic product which can be associated both with the formation of numerous nucleation centers and the thermodynamic factors. It should be noted that an increase of the treatment time, even up to 100 hours at "low" temperature, does not result in the formation of a pure monoclinic phase (Pr3 and Pr4).

The influence of the synthesis temperature on the morphology and size of lanthanum orthophosphate particles can be traced in more details. The temperature lowering (with constant treatment time) from 200 °C (La1) – 160 °C (La3) to 120 °C (La4) leads to a decrease in the particle size, the origination of more defective particle surface and the large deviation in the grain size and, finally, the formation of a second phase (see Table 1, Fig. 3). From SEM images, we can visualize the transformation of the product morphologies over several treatment times and temperatures.

To summarize the results of the given "time-temperature" treatment, one can conclude that the final phase composition strongly depends on the treatment temperature, while the particle size and the degree of crystallinity for the samples are equally influenced by both the synthesis temperature and the time.

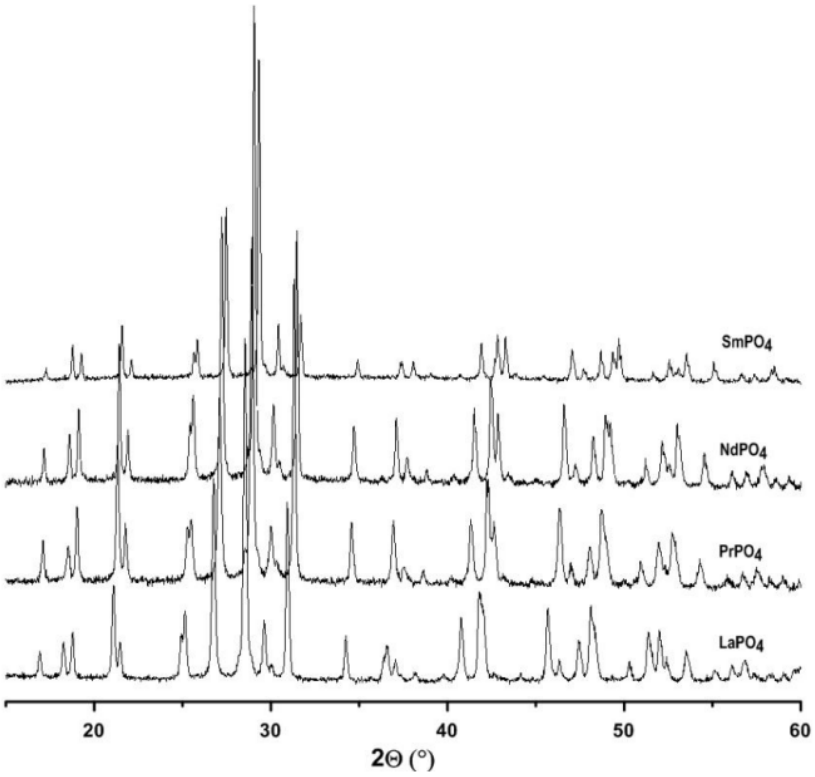

FIG. 1. X-ray diffraction patterns of $LnPO_4$ (Ln = La, Pr, Nd, Sm) synthesized at 200 °C/55 h

TABLE 2. The comparison of unit cell parameters of samples synthesized at 200 °C/55 h with literature data

Substance	*a*, Å	*b*, Å	*c*, Å	*B*, °	*V*, Å^3	Reference
$LaPO_4$	**6.8485(31)**	**7.0818(40)**	**6.5085(31)**	**103.431(37)**	**307.02(27)**	**La1**
Isometric	6.8406(1)	7.0736(1)	6.5126(1)	103.310(1)	306.7(3)	[35]
Isometric	6.841(2)	7.079(3)	6.508(4)	103.33(7)	306.7(4)	[36]
Single crystal	6.8313(10)	7.0705(9)	6.5034(9)	103.27(1)	305.7(5)	[9]
$PrPO_4$	**6.7721(42)**	**6.9938(34)**	**6.4374(49)**	**103.728(58)**	**296.18(33)**	**Pr1**
Isometric	6.7687(5)	6.9900(3)	6.4439(4)	103.5(1)	296.0(5)	[37]
Single crystal	6.4304(4)	6.9785(5)	6.7623(5)	103.516(1)	295.05(4)	[38]
Single crystal	6.741(3)	6.961(4)	6.416(3)	103.63(3)	292.6(5)	[39]
$NdPO_4$	**6.7546(69)**	**6.9725(79)**	**6.4169(65)**	**103.770(79)**	**293.53(54)**	**Nd1**
Isometric	6.7392(9)	6.9621(6)	6.4053(6)	103.6(1)	292.1(4)	[37]
Isometric	6.7426(3)	6.9574(2)	6.4097(3)	103.6624(3)	292.2(3)	[40]
Single crystal	6.722(1)	6.933(1)	6.390(2)	103.72(2)	289.3(2)	[39]
$SmPO_4$	**6.7027(38)**	**6.9068(24)**	**6.3723(30)**	**103.930(50)**	**286.33(24)**	**Sm1**
Isometric	6.6891(3)	6.8958(3)	6.3770(6)	103.9(1)	285.5(3)	[37]
Single crystal	6.6818(12)	6.8877(9)	6.3653(9)	103.86(1)	284.4(5)	[9]
Single crystal	6.669(1)	6.868(2)	6.351(1)	103.92(2)	282.4(2)	[41]

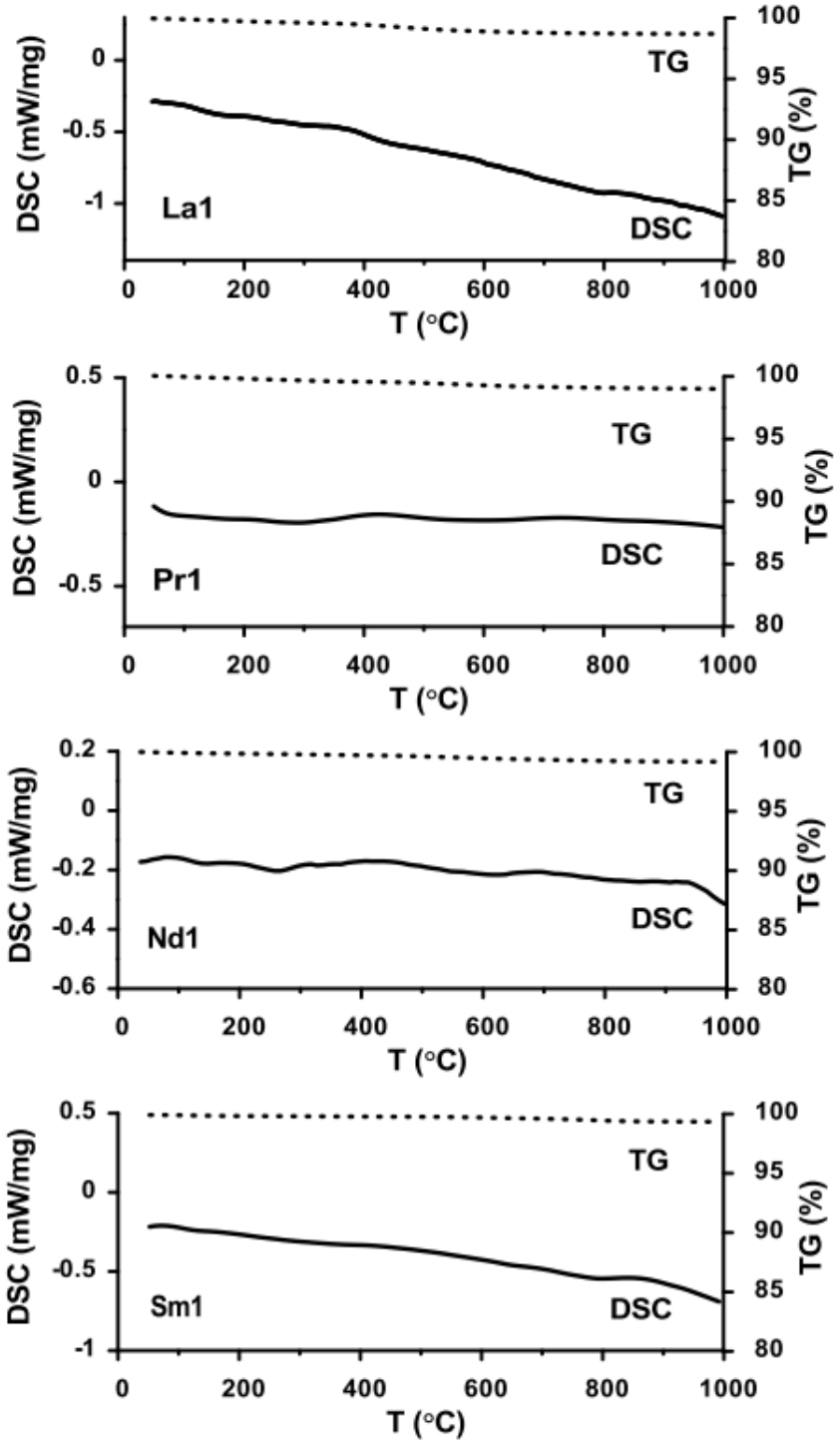

FIG. 2. DSC/TG plots of $LnPO_4$ (Ln = La, Pr, Nd, Sm) synthesized at 200 °C/55 h

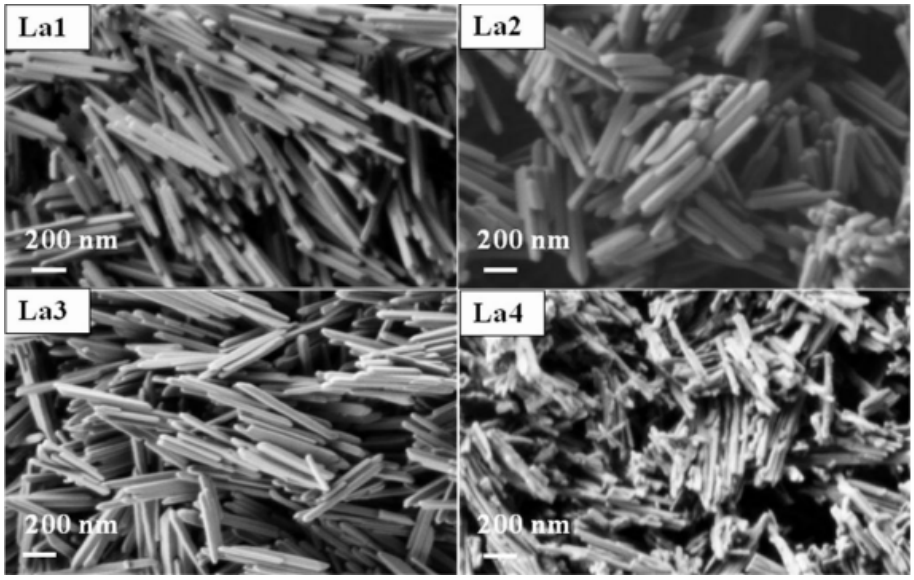

FIG. 3. SEM images of LaPO4 synthesized at several conditions (°C/τ, h): 1 – 200/55, 2 – 200/100, 3 – 160/55, 4 – 120/55

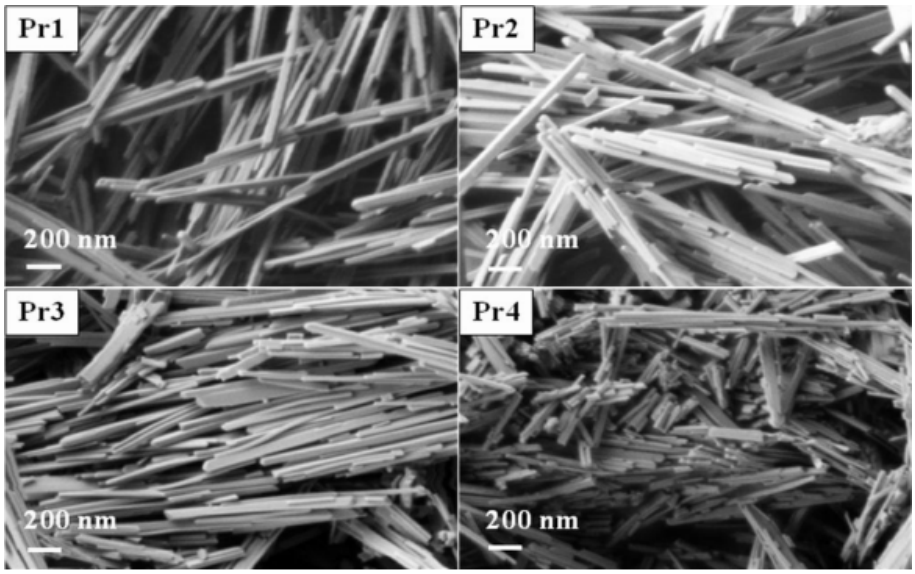

FIG. 4. SEM images of $PrPO_4$ synthesized at several conditions (°C/τ, h): 1 – 200/55, 2 — 200/100, 3 – 160/55, 4 – 160/55

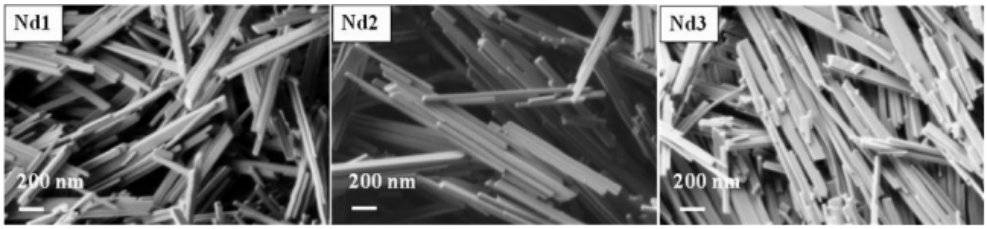

FIG. 5. SEM images of $NdPO_4$ synthesized at several conditions (°C/τ, h): 1 – 200/55, 2 – 200/100, 3 – 160/100

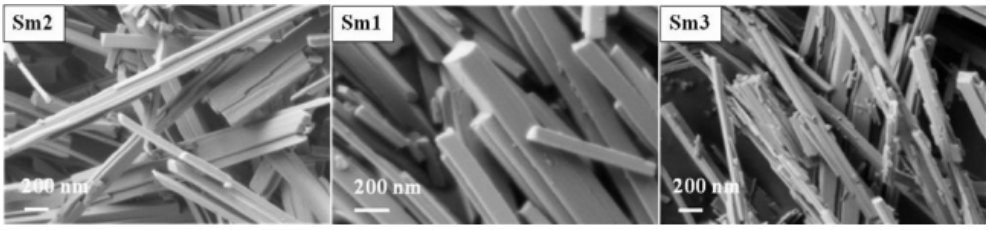

FIG. 6. SEM images of $SmPO_4$ synthesized at several conditions (°C/τ, h): 1 – 200/55, 2 — 200/100, 3 – 160/100

4. Conclusions

The hydrothermal synthesis conditions for the preparation of monoclinic $LaPO_4$, $PrPO_4$, $NdPO_4$ and $SmPO_4$ nanowhiskers without any surface and crystal water has been elaborated. The relationship of the size and morphology of the obtained nanoparticles with the treatment time and temperature was revealed.

Acknowledgements

This work was performed using the equipment of the Joint Research Centre of IGIC RAS.

This study was carried out as the part of the State Assignment on fundamental researches of the Kurnakov Institute of General and Inorganic Chemistry and Research program of the Presidium of the Russian academy of sciences "Scientific foundations of new functional materials production".

References

[1] Guan H., Zhang Y. Hydrothermal synthesis and characterization of hexagonal and monoclinic neodymium orthophosphate single-crystal nanowires. *J. Solid State Chem.*, 2004, **177**(3), P. 781–785.

[2] Yan R., Sun X., et al. Crystal structures, anisotropic growth, and optical properties: controlled synthesis of lanthanide orthophosphate one-dimensional ananomaterials. *Chemistry*, 2005, **11**(7), P. 2183–95.

[3] Yan Z.-G., Zhang Y.-W., et al. General synthesis and characterization of monocrystalline 1D-nanomaterials of hexagonal and orthorhombic lanthanide orthophosphate hydrate. *J. Cryst. Growth*, 2004, **262**(1–4), P. 408–414.

[4] Yu L., Li D., et al. Dependence of morphology and photoluminescent properties of $GdPO_4:Eu^{3+}$ nanostructures on synthesis condition. *Chem. Phys.*, 2006, **326**(2–3), P. 478–482.

[5] Yu L., Song H., et al. Electronic transition and energy transfer processes in $LaPO_4$–Ce^{3+}/Tb^{3+} nanowires. *J. Phys. Chem. B*, 2005, **109**(23), P. 114505.

[6] Lin S., Dong X., Jia R., Yuan Y. Controllable synthesis and luminescence property of $LnPO_4$ (Ln = La, Gd, Y) nanocrystals. *J. Mater. Sci. Mater. Electron.*, 2010, **21**(1), P. 38–44.

[7] Mooney R. C. L. X-ray diffraction study of cerous phosphate and related crystals. I. Hexagonal modification. *Acta Crystallogr.*,1950, **3**(5), P. 337–340.

[8] Fang Y.-P., Xu A.-W., et al. Systematic synthesis and characterization of single-crystal lanthanide orthophosphate nanowires. *J. Am. Chem. Soc.*, 2003, **125**(51), P. 16025–16034.

[9] Ni Y., Hughes J.M., et al. Crystal chemistry of the monazite and xenotime structures. *Am. Mineralogist*, 1995, **80**, P. 21–26.

[10] Bühler G., Feldmann C. Microwave-assisted synthesis of luminescent $LaPO_4$: Ce,Tb nanocrystals in ionic liquids. *Angew. Chem. Int. Ed. Engl.*, 2006, **45**(29), P. 48647.

[11] Brown S.S., Im H.-J., Rondinone A.J., Dai S. Facile, alternative synthesis of lanthanum phosphate nanocrystals by ultrasonication. *J. Colloid Interface Sci.*, 2005, **292**(1), P. 127–132.

[12] Yu C., Yu M., et al. Facile sonochemical synthesis and photoluminescent properties of lanthanide orthophosphate nanoparticles. *J. Solid State Chem.*, 2009, **182**, P. 339–347.

[13] Diaz-Guillén J.A., Fuentes A.F., Gallini S., Colomer M.T. A rapid method to obtain nanometric particles of rhabdophane $LaPO_4 \cdot nH_2O$ by mechanical milling. *J. Alloys Compd.*, 2007, **427**(1–2), P. 87–93.

[14] Bregiroux D., Audubert F., et al. Solid-state synthesis of monazite-type compounds $LnPO_4$ (Ln = La to Gd). *Solid State Sci.*, 2007, **9**(5), P. 432–439.

[15] Kijkowska R. Preparation of lanthanide orthophosphates. *J. Mater. Sci.*, 2003, **8**(38), P. 229-233.

[16] Boakye E.E., Mogilevsky P., Hay R.S. Synthesis of Nanosized Spherical Rhabdophane Particles. *J. Am. Ceram. Soc.*, 2005, **88**(10), P. 2740–46.

[17] Gavrichev K.S., Ryumin M.A., et al. Thermal behavior of $LaPO_4 \cdot nH_2O$ and $NdPO_4 \cdot nH_2O$ nanopowders. *J. Therm. Anal. Calorim.*, 2010, **102**(2), P. 809–811.

[18] Li L., Jiang W., et al. Improved Luminescence of Lanthanide(III)-Doped Nanophosphors by Linear Aggregation. *J. Phys. Chem. C*, 2007, **111**, P. 4111–15.

[19] Ruigang W., Wei P., et al. Synthesis and sintering of $LaPO_4$ powder and its application. *Mater. Chem. Phys.*, 2003, **79**(1), P. 30–36.

[20] Chen P., Mah T. Synthesis and characterization of lanthanum phosphate sol for fibre coating. *J. Mater. Sci.*, 1997, **32**(14), P. 3863–67.

[21] Buissette V., Moreau M., et al. Colloidal Synthesis of Luminescent Rhabdophane $LaPO_4:Ln^{3+} \cdot xH_2O$ (Ln = Ce, Tb, Eu, $x \approx 0.7$) *Nanocrystals. Chem. Mater.*, 2004, **16**(19), P. 3767–73.

[22] Kijkowska R. Thermal decomposition of lanthanide orthophosphates synthesized through crystallisation from phosphoric acid solution. *Thermochim. Acta*, 2003, **404**(1–2), P. 81–88.
[23] Yu M., Lin J., et al. Sol-gel synthesis and photoluminescent properties of $LaPO_4$:A (A = Eu^{3+}, Ce^{3+}, Tb^{3+}) nanocrystalline thin films. *J. Mater. Chem.*, 2003, **13**(6), P. 1413–19.
[24] Byrappa K. Preparative methods and growth of rare earth phosphates. *Prog. Cryst. Growth Charact.*, 1986, **13**(3), P. 163–196.
[25] Bao J.R., Zhu X.W., et al. Hydrothermal Synthesis of Neodymium Orthophosphate with Controlled Structure and Morphology. *Adv. Mater. Res.*, 2012, **399–401**, P. 635–640.
[26] Onoda H., Nariai H., et al. Formation and catalytic characterization of various rare earth phosphates. *J. Mater. Chem.*, 2002, **12**(6), P. 1754–60.
[27] Peng Z.A., Peng X. Nearly Monodisperse and Shape-Controlled CdSe Nanocrystals via Alternative Routes: Nucleation and Growth. *J. Am. Chem. Soc.*, 2002, **124**(13), P. 3343–53.
[28] Zhang Y.-W., Yan Z.-G., et al. General Synthesis and Characterization of Monocrystalline Lanthanide Orthophosphate Nanowires. *Eur. J. Inorg. Chem.*, 2003, **2003**(22), P. 4099–4104.
[29] Zhang Y., Guan H. The growth of lanthanum phosphate (rhabdophane) nanofibers via the hydrothermal method. *Mater. Res. Bull.*, 2005, **40**(9), P. 1536–43.
[30] Dong H., Liu Y., et al. Controlled synthesis and characterization of $LaPO_4$, $LaPO_4$:Ce^{3+} and $LaPO_4$:Ce^{3+}, Tb^{3+} by EDTA assisted hydrothermal method. *Solid State Sci.*, 2010, **12**(9), P. 1652–60.
[31] Wang X., Li Y. Synthesis and characterization of lanthanide hydroxide single-crystal nanowires. *Angew. Chem. Int. Ed. Engl.*, 2002, **41**(24), P. 4790–93.
[32] Ma J., Wu Q. A novel additive-free oxideshydrothermal approach for monazite-type $LaPO_4$ nanomaterials with controllable morphologies. *J. Appl. Crystallogr.*, 2010, **43**(5), P. 990–997.
[33] Byrappa K., Devaraju M.K., et al. Hydrothermal synthesis and characterization of $LaPO_4$ for bio-imaging phosphors. *J. Mater. Sci.*, 2008, **43**(7), P. 2229–33.
[34] Yang M., You H., et al. Selective synthesis of hexagonal and monoclinic $LaPO_4$:Eu^{3+} nanorods by a hydrothermal method. *J. Cryst. Growth*, 2009, **311**(23–24), P. 4753–58.
[35] Thiriet C., Konings R.J.M., Javorský P., Magnani N. The low temperature heat capacity of $LaPO_4$ and $GdPO_4$, the thermodynamic functions of the monazite-type $LnPO_4$ series. *J. Chem. Thermodyn.*, 2005, **37**(2), P. 131–139.
[36] Terra O., Clavier N., Dacheux N., Podor R. Preparation and characterization of lanthanum-gadolinium monazites as ceramics for radioactive waste storage. *New J. Chem.*, 2003, **27**(6), P. 957–967.
[37] Ushakov S., Helean K. Thermochemistry of rare-earth orthophosphates. *J. Mater. Res.*, 2001, **16**(100), P. 2623–33.
[38] Horchani-Naifer K., Férid M. Crystal structure, energy band and optical characterizations of praseodymium monophosphate $PrPO_4$. *Inorganica Chim. Acta*, 2009, **362**(6), P. 1793–96.
[39] Mullica D.F., Grossie D., Boatner L.A. Structural refinements of praseodymium and neodymium orthophosphate. *J. Solid State Chem.*, 1985, **58**(1), P. 71–77.
[40] Jardin R., Pavel C.C., et al. The high-temperature behaviour of $PuPO_4$ monazite and some other related compounds. *J. Nucl. Mater.*, 2008, **378**(2), P. 167–171.
[41] Mullica D.F., Grossie D., Boatner L.A. Coordination geometry and structural determinations of $SmPO_4$, EuPO4 and GdPO4. *Inorganica Chim. Acta*, 1985, **109**(2), P. 105–110.